

Title

A comprehensive study on the effect of cavitation on injection velocity in diesel nozzles.

Authors

- (1) J. Javier López, F. Javier Salvador and Oscar de la Garza.
- (2) Jean Arrègle.

Affiliation

- (1) CMT-Motores Térmicos
 - (2) Departamento de Máquinas y Motores Térmicos
- Universidad Politécnica de Valencia, Spain
Camino de Vera, s/n. 46022 Valencia, SPAIN

Corresponding author

J. Javier López
CMT-Motores Térmicos
Universidad Politécnica de Valencia
Camino de Vera, s/n. 46022 Valencia, SPAIN
e-mail: jolosan3@mot.upv.es
Tlf: +34 963 879 232, Fax: +34 963 877 659

Abstract

Results when testing cavitating injection nozzles show a strong reduction in mass flow rate when cavitation appears (the flow is choked), while the momentum flux is reduced to a lesser extent, resulting in an increase in effective injection velocity. So as to better understand the origin of this increase in effective injection velocity, the basic equations for mass and momentum conservation were applied to an injection nozzle in simplified conditions.

The study allowed to demonstrate that the increase in injection velocity provoked by cavitation is not a *direct* effect of the latter, but an *indirect* effect. In fact, the vapor appearance inside the injection hole produces a decrease in the viscosity of the fluid near the wall. This leads to lower momentum flux losses and to a change in the velocity profile, transforming it into a more “top hat” profile type. This change in the profile shape allows explaining why the momentum flux reduction is not so important compared to that of the mass flow rate, thus explaining why the effective injection velocity increases.

Keywords

Nozzle cavitation, velocity profile, injection velocity.

1 Introduction

The design of the injection nozzle in a diesel engine is an important factor to improve the combustion process and, above all, to reduce pollutant emissions, because the nozzle geometry has an influence on the spray characteristics, particularly in its mixing process [1,2]. This is the main reason why there are lots of studies analyzing the effect of nozzle geometry on its internal and external flow [3,4]. One of the aspects the nozzle geometry has an influence on is the appearance or not of the cavitation phenomenon. It is well-

known that even if this phenomenon has a clear negative effect on the permeability, it also has a positive effect on the atomization [5,6] and the mixing process [2,7]. For this reason it has been widely studied.

The effect of cavitation on the flow in an injection nozzle usually has been analyzed in terms of what happens with the mass flow rate. Concerning this parameter, it can be stated that it is significantly reduced by cavitation. In fact, the mass flow rate reaches choking conditions when the injection pressure is kept constant and the back-pressure is reduced below a certain limit, as shown in Fig.1 using some results already published [8]. In those experiments 5 different injection pressure levels were used, and for each of them the back-pressure was modified. Figure 1 shows, on the one hand, results corresponding to a conical nozzle (i.e. without cavitation) and a cylindrical nozzle (i.e. with cavitation under some working conditions), both having a similar Bosch Flow Number¹. The Figure also shows, on the other hand, the evolution of the mass flow rate (to the left) and the discharge coefficient (to the right) of both nozzles. The discharge coefficient is defined as follows:

$$C_d = \frac{\dot{m}}{\rho_L \cdot A_o \cdot u_{berno}} \quad (1)$$

where \dot{m} is the mass flow rate, ρ_L is the density of the liquid fuel, A_o is the geometric cross-sectional area of the orifice, and u_{berno} is the Bernoulli's velocity. In both curves it can be clearly observed the strong effect of cavitation on this aspect (cylindrical nozzle). This is a very common result [5,7,9], and its justification has been known for more than 30 years [7]. In that work, Nurick states that when the vapor pressure is achieved at the minimum area orifice section, this pressure level can not be reduced anymore even if the pressure at the discharge enclosure is further reduced. This fact, similarly as what

¹This parameter represents the volume of fuel injected during 30 seconds using an injection pressure and a back-pressure of 10 and 0.1 MPa, respectively. It is worthy to underline that a lot of cavitation exists in the cylindrical nozzle under these conditions, and consequently the permeability of this nozzle will be much higher than the other when there is no cavitation.

happens in a convergent-divergent nozzle where the sonic conditions at the “throat” are achieved, lead to blocking the mass flow rate.

In Fig.1, to the right, it can be clearly observed that the flow through a nozzle (quantified by the C_d) depends both on the Re and on the cavitation level, usually quantified by the Nurick Cavitation Number, K , defined as follows:

$$K = \frac{p_{inj} - p_{vap}}{p_{inj} - p_{back}} \quad (2)$$

where p_{inj} is the injection pressure, p_{back} is the back-pressure, and p_{vap} is the fuel vapor pressure. If the experimental procedure commonly used for the study of cavitation (to keep a constant injection pressure modifying only the back-pressure) is analyzed in a critical way, it can be seen that both Re and K are changed at the same time. A better way to proceed to study cavitation is to change only K while keeping a constant Re . This can be done working at a constant Δp ($p_{inj} - p_{back}$), i.e. modifying p_{inj} and p_{back} at the same time.

When working with this methodology with different nozzles and injectors, it is observed that sometimes the effect of Re on the flow is negligible whereas some other times it is very important. The example that will be used in a moment to more deeply show the effect of cavitation on the flow, corresponds to two nozzles (a conical and a cylindrical nozzle) with a single orifice in which the Re is not important at all. This way we can focus our attention on the effect of K , i.e. on cavitation.

Some measurements of the mass flow rate and momentum flux have been performed with these two nozzles, as had been already done in many previous studies using the traditional methodology [8, 10]. When analyzing the momentum flux, a momentum coefficient is defined (in a similar way to the discharge coefficient for the mass flow rate) as follows:

$$C_M = \frac{\dot{M}}{\rho_L \cdot A_o \cdot u_{berno}^2} \quad (3)$$

where \dot{M} is the momentum flux. From these two coefficients (C_d and C_M), the velocity

coefficient relating the effective velocity and the Bernoulli's velocity can be defined:

$$u_{ef} = \frac{\dot{M}}{\dot{m}} = C_v \cdot u_{berno} \quad \Rightarrow \quad C_v = \frac{C_M}{C_d} \quad (4)$$

In Fig.2 the value for these three coefficients is shown only for the cylindrical nozzle (the case where cavitation can appear). The different data have been presented in the following way: each coefficient has been divided by its corresponding value when there is no cavitation, in such a way that they have a value of 1 in the non-cavitating region. From this Figure, it can be observed that:

- The mass flow rate, represented by C_d , is strongly reduced as the cavitation intensity increases (i.e. as K approaches the value 1).
- The momentum flux, represented by C_M , is also reduced as the cavitation intensity increases, but to a lesser extent compared to the mass flow rate.
- As a consequence of the two previous points, the effective injection velocity, represented by C_v , increases as the cavitation intensity increases.

As a conclusion, cavitation provokes an increase in injection velocity. The objective of this work is to analyze the causes for this increase, trying to find out if it is a *direct* consequence of cavitation or if it is an *indirect* consequence, i.e. that cavitation produces some changes in the fluid that would lead, as a secondary consequence, to an increase in velocity.

To perform this study a very simplified case (in order to allow for an analytical solution) will be analyzed to find out which are the “expected” theoretical effects (i.e. *direct* effects) of cavitation on flow velocity. This result will be then compared to some CFD results and some experimental results to try to better understand the mechanisms of the effect of cavitation on the flow velocity.

2 Theoretical analysis of the *direct* effects of cavitation

Because of the enormous difficulty when trying to analytically solve a cavitating flow in a nozzle, the theoretical analysis that will be performed here is going to be done in a very simplified case. Further in this study the validity and scope of the results obtained here will be discussed. This analysis is closely related to the one performed by Nurick [7] and the one performed later by Schmidt and Corradini [11]. The main hypotheses are the following:

- An orifice configuration as the one shown in Fig.3 is assumed. It is worthy to underline that the orifice (geometrically cylindrical), because of the fluid dynamics, presents a narrowing provoked by a recirculation zone that makes it similar to a convergent-divergent nozzle (independently of the existence or not of cavitation). Three interesting cross-sections have been marked in the Figure: section 1, at the inlet, where the velocity is negligible; section c , at the narrowing, where the cross-sectional area has the minimum value; and section 2, at the exit of the orifice.
- The fluid and flow properties are assumed to be uniform at each section.
- Friction between the fluid and the wall is neglected.
- The cavitating case to be analyzed will be the one where $p_2 = p_{vap}$.

The only equations to be used are the continuity equation, the momentum theorem and the energy equation. The latter, if particularized to an incompressible fluid translates into the Bernoulli's theorem (obviously, this equation can only be used in the regions where no biphasic flow exists).

To perform the theoretical analysis, a cavitating case will be compared to a non-cavitating one. The particular cavitating case, as mentioned above, is the one where the pressure at the orifice outlet is precisely the vapor pressure (in this case, the pressure

between the throat and the exit is uniform and equal to p_{vap}). The non-cavitating case is a case with the same Δp between the inlet and the outlet, but with a p_c at the throat higher than the vapor pressure (in order to avoid cavitation).

Starting by the non-cavitating case, as no biphasic flow exists in any of the intermediate sections, the mass flow rate and the momentum flux at the outlet section can be directly calculated by using the basic equations for incompressible flow:

$$\dot{m}_{w/o_cav} = \rho_L \cdot A_2 \cdot u_{2_w/o_cav} \quad (5)$$

where u_{2_w/o_cav} can be obtained from Bernoulli's equation:

$$u_{2_w/o_cav} = \left(\frac{2 \cdot (p_1 - p_2)}{\rho_L} \right)^{0.5} \quad (6)$$

$$\dot{M}_{w/o_cav} = \rho_L \cdot A_2 \cdot u_{2_w/o_cav}^2 \quad (7)$$

For the cavitating case, the mass flow rate can be written in the following way:

$$\dot{m}_{w_cav} = \rho_L \cdot A_c \cdot u_{c_w_cav} = \rho_2 \cdot A_2 \cdot u_{2_w_cav} \quad (8)$$

where the value of $u_{c_w_cav}$ can be obtained from Bernoulli's equation (because between section 1 and c there is no biphasic flow):

$$u_{c_w_cav} = \left(\frac{2 \cdot (p_1 - p_c)}{\rho_L} \right)^{0.5} \quad (9)$$

As $p_c = p_2 = p_{vap}$, from Eqs. (6) and (9) it can be deduced that $u_{c_w_cav} = u_{2_w/o_cav}$ (because the pressure difference $p_1 - p_2$ is the same in both cases).

For the momentum flux it can be written:

$$\dot{M}_{w_cav} = \rho_2 \cdot A_2 \cdot u_{2_w_cav}^2 \quad (10)$$

Now, let's try to relate this momentum flux at the exit with the one at the throat, because its value can be known at this latter section. If the momentum theorem is applied between section c and 2 (the control volume considered is shown in Fig.4), we obtain the following (only the pressure forces are taken into account, because friction was considered to be negligible):

$$p_c \cdot A_c - p_2 \cdot A_2 + F_{wall} = \Delta \dot{M} \quad (11)$$

F_{wall} can be obtained as the integration of the pressure forces. The expression can be easily integrated because pressure is constant in all the considered control volume (this is the main reason to select this particular case for the analysis):

$$F_{wall} = \int_c^2 p \cdot dA = p_{vap} \cdot (A_2 - A_c) \quad (12)$$

Substituting Eq. (12) into Eq. (11), taking into account that $p_c = p_2 = p_{vap}$, it is obtained:

$$p_c \cdot A_c - p_2 \cdot A_2 + p_2 \cdot A_2 - p_c \cdot A_c = 0 = \Delta \dot{M} \quad (13)$$

thus deducing that the momentum flux is the same in sections c and 2. Then, Eq. (10) can be written as follows:

$$\dot{M}_{w_cav} = \rho_2 \cdot A_2 \cdot u_{2_w_cav}^2 = \rho_L \cdot A_c \cdot u_{c_w_cav}^2 \quad (14)$$

Taking into account these results, the effect of cavitation on the mass flow rate and the momentum flux can be found. Concerning the mass flow rate, if Eq. (5) is divided by Eq. (8), it is obtained:

$$\frac{\dot{m}_{w/o_cav}}{\dot{m}_{w_cav}} = \frac{\rho_L \cdot A_2 \cdot u_{2_w/o_cav}}{\rho_L \cdot A_c \cdot u_{c_w_cav}} = \frac{A_2}{A_c} \quad (15)$$

And concerning the momentum flux, if Eq. (7) is divided by Eq. (14), it is found:

$$\frac{\dot{M}_{w/o_cav}}{\dot{M}_{w_cav}} = \frac{\rho_L \cdot A_2 \cdot u_{2_w/o_cav}^2}{\rho_L \cdot A_c \cdot u_{c_w_cav}^2} = \frac{A_2}{A_c} \quad (16)$$

As can be seen, the result is the same as for the mass flow rate. Besides, for the cavitating case, as both the mass flow rate and the momentum flux are the same in sections c and 2, it can be deduced that velocity is also the same, and it can be written that $u_{2_w_cav} = u_{c_w_cav} = u_{2_w/o_cav}$.

Consequently, based on the particular case analyzed here, the effect of cavitation on \dot{m} and \dot{M} is theoretically the same, and thus the exit velocity would not be altered. This means that the cavitation process, which translates mainly in a reduction in density due to the appearance of a biphasic flow, does not *directly* produce an increase in flow velocity. Even if this statement is only valid for a very particular case as the one analyzed here (we have proceed like this because to analytically solve the problem in other pressure conditions is extremely more complicated), there is a fact that can help to generalize the result. The case analyzed corresponds to the case where $p_2 = p_{vap}$, and in these conditions the cavitation intensity is huge. If with this level of cavitation, much higher than the one that can be found in a diesel nozzle, there is no increase in velocity, it can be thought that the velocity will not increase for any other lower cavitation level. As a conclusion, even if this theoretical result has been obtained for a very particular case, it seems that the result (that cavitation does not *directly* provoke an increase in the flow velocity) can be considered as a general result.

Once this point has been reached, if cavitation doesn't have a *direct* effect on the increase in effective injection velocity, it is important to wonder which parameter is affected by cavitation that may be responsible for this increase in velocity. The hypothesis to be considered here is that cavitation produces a decrease in fluid viscosity, the effect of which can be observed from two complementary points of view:

- On the one hand, wall friction is reduced where cavitation appears (i.e. between sections c and 2). In the theoretical development just shown above, wall friction has

been neglected so as to be able to obtain an analytical solution for the analyzed case. If this friction were considered, we would found that momentum flux between sections c and 2 would decrease to a lesser extent in the cavitating case compared to the non-cavitating case, which would explain why the momentum flux reduction is actually smaller compared to what ideally (i.e. without friction) would be expected.

- On the other hand, the decrease in viscosity leads to an increase in Re , thus increasing the turbulent character of the flow. This would lead to a transformation of the velocity profile towards a more “top hat” shape (velocity will keep a higher value near the wall). This change in the velocity profile, which is in fact related to what has been explained in the previous item, is what can explain why the decrease in mass flow rate and in momentum flux is not the same.

The effect of the fluid viscosity on the velocity profile (i.e. the latter point of view) will be analyzed in next section.

3 Analysis of the effect of viscosity (*without cavitation*) on the velocity profile

It has just been said that the viscosity drop caused by cavitation would lead to a more “top hat” velocity profile. This change in the velocity profile shape could possibly explain that the effect of cavitation on \dot{m} (which is proportional to $\int u$) and on \dot{M} (proportional to $\int u^2$) would be different.

In order to validate this hypothesis, some simulations with the CFD code FLUENT [12] will be used. The main characteristics and parameters for the simulations are summarized in Table 1. The effect of the fluid viscosity (of *all* the fluid, i.e. not considering biphasic flow) on the flow through a convergent (so as to avoid cavitation and, consequently, a biphasic flow), single-orifice nozzle was studied. The orifice diameter was $112\ \mu m$ and its length was $1\ mm$. The turbulence model was a $k - \varepsilon$ RNG model, with

standard values for the different parameters. For the calculations, an injection pressure of 71 MPa and a back-pressure of 1 MPa were considered, and the velocity profiles at the outlet section for three different viscosity values were compared:

- $3.67 \cdot 10^{-3} \text{ kg}/(\text{m} \cdot \text{s})$ (corresponding to liquid diesel fuel),
- $7.34 \cdot 10^{-4} \text{ kg}/(\text{m} \cdot \text{s})$ (80% smaller than that of the liquid diesel fuel, which would correspond to the viscosity of a blend of liquid and vapor diesel fuel with a vapor mass fraction of 0.8, as explained later), and
- $1.829 \cdot 10^{-4} \text{ kg}/(\text{m} \cdot \text{s})$ (95% smaller than that of the liquid diesel fuel, corresponding to the viscosity of a blend of liquid and vapor diesel fuel with a vapor mass fraction of 0.95).

For determining these viscosity levels, the method currently used in commercial CFD codes was used, i.e. assuming that the viscosity of a blend is the weighted average, as a function of the vapor mass fraction, of the liquid and vapor viscosity: $\mu_m = \mu_L \cdot (1 - Y_{vap}) + \mu_{vap} \cdot Y_{vap}$. The authors are aware of the unlikely hypothesis laying behind this method, but the validity of this common way for computing the viscosity of a liquid-vapor blend is out of the scope of this paper.

In Fig. 5, the effective viscosity profile at the outlet section as a function of the normalized radial coordinate (ξ , defined as the ratio between r , the radial coordinate, and R , the radius) is shown. It can be observed that the effective viscosity values approximately keep the magnitude of the introduced laminar viscosities, and thus the viscosity levels are the ones previously searched. In Fig. 6, the velocity profiles for the three corresponding cases are shown. It can be clearly observed that viscosity affects very significantly the velocity profile and in the expected way: as the viscosity is reduced, the profile is more similar to a “top hat” profile.

For these three obtained profiles, the effective velocity value, computed as \dot{M}/\dot{m} , was obtained. The results are shown in Table 2 (both absolute and relative –respect

to the higher viscosity case— results are given). The obtained values are similar to the experimental results previously shown (Fig. 2). It can be stated, then, that the formulated hypothesis (that there is a change in the velocity profile caused by the variation in viscosity produced by cavitation) can suitably explain the experimental results: cavitation has a stronger effect on \dot{m} than on \dot{M} , thus increasing the effective velocity at the nozzle exit.

When viewing these results, a possible criticism that can be launched is that the viscosity variation that leads to a significant alteration of the velocity profile that, in turn, produces an increase in injection velocity similar to the one obtained experimentally is excessively high. Here it is important to point out that in these simulations the viscosity drop (which in the real case is associated to the appearance of vapor) is introduced uniformly in the whole section, whereas in the real case the vapor generated by cavitation is mostly concentrated near the walls [13,14]. Consequently, for *global* vapor mass fractions relatively small and coherent with experimental results, the *local* vapor mass fraction near the wall and the corresponding viscosity drop are much more important. Besides, the viscosity near the wall is the one responsible for the change in velocity profile (because this one changes mostly in the region near the wall). This is what will be validated in the next section.

4 Analysis of the effect of *local* variations in vapor mass fraction and viscosity on the velocity profile

Finally, trying to enlarge the validity of the results obtained up to now, some simulations with the CFD code Star-CD were performed, using a cavitation model based on the Rayleigh equation [15,16]. In the two simulated cases the pressure drop across the orifice was kept constant, thus maintaining the Reynolds number. In Fig. 7, the velocity profiles at the orifice outlet are shown for two cases: one with an injection pressure of 80 MPa and a back-pressure of 10 MPa (without cavitation) and the other with an injection pressure of 71 MPa and a back-pressure of 1 MPa (with cavitation). It can be observed that the

trend is exactly the same as the one previously observed and discussed, reinforcing the result.

In Figs. 8 and 9, the radial evolution of the vapor mass fraction inside the nozzle and the effective viscosity for the same cases already shown in Fig. 7 are presented, respectively. It can be observed that the change in the velocity profile, which is comparable to the one observed when changing the viscosity in the whole section, can be explained by the viscosity variation caused by cavitation, which only takes place near the wall.

To conclude the analysis, these CFD results will be compared with the experimental data already shown in Fig.2. The comparison will be performed as follows: the increase in velocity (characterized by the C_v coefficient) will be plotted as a function of a parameter related to the cavitation intensity (which is the cause for this increase in velocity), characterized e.g. by the C_d coefficient. The same information previously shown in Fig.2 is now presented in this new way in Fig.10. In this Figure, the same information corresponding to the CFD simulations are also shown. It can be observed that the simulation agrees with the experiments, thus supporting the results of all the analysis presented in the paper.

5 Conclusions

The main conclusions at the end of this study are the following:

- Cavitation has a direct effect on the fuel mass flow rate, which is significantly reduced because of the choke produced by cavitation.
- Experimentally it is observed that the momentum flux is also reduced due to cavitation, but to a lesser extent compared to the mass flow rate. This fact, together with the previous one, leads to an increase in effective injection velocity.
- The theoretical development applied to the simplified case studied here shows that cavitation does not have a *direct* effect on the effective injection velocity (because, in principle, it wouldn't be modified). But as a biphasic flow exists, the behavior

is much more complex. In fact, as some vapor appears near the orifice walls, the fluid viscosity reduces, thus diminishing friction. This has a consequence that can be looked at from two complementary points of view: (1) there are less losses of momentum flux in this region of the nozzle, and (2) the velocity profile is modified, changing to a more “top hat” shape. This change in the velocity profile can harmonize an important reduction in mass flow rate with a less important decrease in momentum flux, in such a way that the effective injection velocity, i.e. the ratio of these two magnitudes, increases (in agreement with the experimental observations).

Acknowledgements

We thank different members of the CMT-Motores Térmicos team for their contribution to this work: to Jaime Gimeno, for his fruitful comments, and to Xandra Margot, Stavroula Patouna and Gabriela Bracho for their help in the CFD calculations.

FLUENT and Star-CD are registered trademarks of ANSYS and CD Adapco, respectively.

Notation

A	Cross-sectional area
C_d	Discharge coefficient
CFD	Computational Fluid Dynamics
C_M	Momentum flux coefficient
C_v	Velocity coefficient
F	Force
K	Nurick Cavitation Number $(\frac{p_{inj}-p_{vap}}{p_{inj}-p_{back}})$
\dot{m}	Mass flow rate

\dot{M}	Momentum flux
p	Pressure
r	Radial coordinate
R	Radius
Re	Reynolds number
RNG	ReNormalization Group
u	Velocity
Y	Mass fraction

Greek symbols

Δp	Pressure drop
μ	Dynamic viscosity
ξ	Normalized radial coordinate (r/R)

Subscripts

1, 2	In sections 1, 2
<i>back</i>	In the enclosure where the fuel is injected
<i>berno</i>	Referred to Bernoulli (theoretical)
<i>c</i>	In section <i>c</i> (minimum cross-sectional area)
<i>inj</i>	Referred to injection
<i>L</i>	Referred to liquid
<i>m</i>	Referred to the mixture
<i>NC</i>	No Cavitation
<i>o</i>	At the orifice exit

<i>vap</i>	Referred to vapor
<i>w_cav</i>	With cavitation
<i>w/o_cav</i>	Without cavitation
<i>wall</i>	Referred to the wall

References

1. Kampmann, S., Dittus, B., Mattes, P., and Kirner, M., 1996. “The influence of hydro grinding at vco nozzles on the mixture preparation in a di diesel engine”. *SAE Paper 960867*.
2. Payri, R., Salvador, F., Gimeno, J., and Zapata, D., 2008. “Diesel nozzle geometry influence on spray liquid-phase fuel penetration in evaporative conditions”. *Fuel*, **87**, pp. 1165–1176.
3. Kent, J., and Brown, G., 1983. “Nozzle exit flow characteristics for square-edged and rounded inlet geometries”. *Combustion Science and Technology*, **30**, pp. 121–132.
4. Payri, R., Molina, S., Salvador, F., and Gimeno, J., 2004. “A study of the relation between nozzle geometry, internal flow and spray characteristics in diesel fuel injection system”. *KMSM International Journal*, **18**(7), pp. 1222–1235.
5. Soteriou, C., Andrews, R., and Smith, M., 1995. “Direct injection diesel sprays and the effect of cavitation and hydraulic flip on atomization”. *SAE Paper 950080*.
6. Suh, H., and Lee, C., 2008. “Effect of cavitation in nozzle orifice on the diesel fuel atomization characteristics”. *International Journal of Heat and Fluid Flow*, **29**, pp. 1001–1009.
7. Nurick, W., 1976. “Orifice cavitation and its effect on spray mixing”. *Journal of Fluids Engineering*, **98**, pp. 681–687.

8. Payri, R., García, J., Salvador, F., and Gimeno, J., 2005. “Using spray momentum flux measurements to understand the influence of diesel nozzle geometry on spray characteristics”. *Fuel*, **84**, pp. 551–561.
9. Payri, R., Salvador, F., Gimeno, J., and de la Morena, J., 2009. “Study of cavitation phenomena based on a technique for visualizing bubbles in a liquid pressurized chamber”. *International Journal of Heat and Fluid Flow*, **30**, pp. 768–777.
10. Desantes, J., Arrègle, J., López, J., and Hermens, S., 2005. “Experimental characterization of outlet flow for different diesel nozzle geometries”. *SAE Paper 2005-01-2120*.
11. Schmidt, D., and Corradini, M., 1997. “Analytical prediction of the exit flow of cavitating orifices”. *Atomization and Sprays*, **7**(6), pp. 603–616.
12. Fluent, 2001. *FLUENT: User’s Guide*. Fluent Incorporated.
13. Soteriou, C., Andrews, R., and Smith, M., 1999. “Further studies of cavitation and atomization in diesel injection”. *SAE Paper 1999-01-1486*.
14. Som, S., Aggarwal, S., El-Hannouny, E., and Longman, D., 2010. “Investigation of nozzle flow and cavitation characteristics in a diesel injector”. *Journal of Engineering for Gas Turbines and Power*, **132**, pp. –.
15. Rayleigh, L., 1917. “On the pressure developed in a liquid during the collapse of a spherical cavity”. *Philosophical Magazine*, **34**, pp. 94–98.
16. Payri, F., Margot, X., Patouna, S., Ravet, F., and Funk, M., 2009. “A cfd study of the effect of the needle movement on the cavitation pattern of diesel injectors”. *SAE Paper 2009-24-0025*.

List of Figures

1	Results for a cylindrical (cavitating) and conical (non-cavitating) nozzle with identical Bosch Flow Number. Left.- Mass flow rate as a function of $\Delta p^{0.5}$. Right.- Discharge coefficient (C_d) as a function of Re	19
2	Evolution of C_d , C_M and C_v for a cylindrical nozzle (i.e. a potentially cavitating nozzle). The values have been normalized by the corresponding non-cavitating value.	20
3	Schematics of the orifice configuration.	21
4	Control volume between sections c and 2.	22
5	Effective viscosity profiles as a function of the normalized radial coordinate for the three viscosity levels simulated.	23
6	Velocity profiles as a function of the normalized radial coordinate for the three viscosity levels simulated.	24
7	Velocity profiles as a function of the normalized radial coordinate for a cavitating and a non-cavitating case, both simulated with Star-CD using a cavitation model based in the Rayleigh equation.	25
8	Evolution of the vapor mass fraction as a function of the normalized radial coordinate for the cases shown in Fig. 7.	26
9	Evolution of the effective viscosity as a function of the normalized radial coordinate for the cases shown in Fig. 7.	27
10	C_v versus C_d variations for the experimental cases shown in Fig.2. The same information for the CFD results is also shown.	28

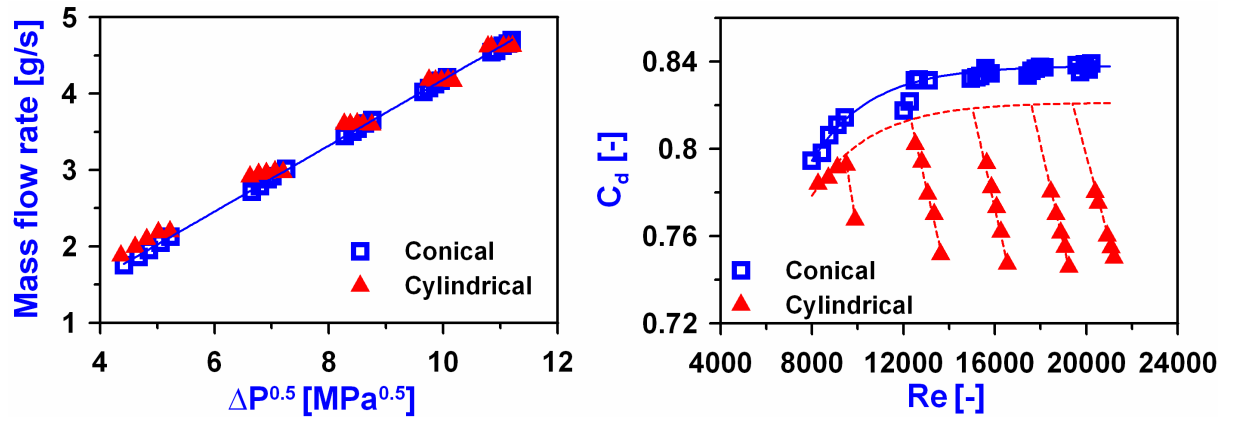


Figure 1: Results for a cylindrical (cavitating) and conical (non-cavitating) nozzle with identical Bosch Flow Number. **Left.-** Mass flow rate as a function of $\Delta p^{0.5}$. **Right.-** Discharge coefficient (C_d) as a function of Re .

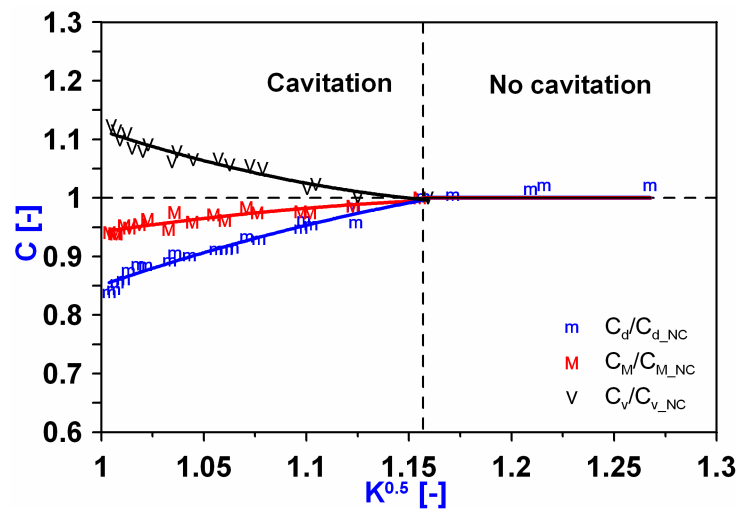


Figure 2: Evolution of C_d , C_M and C_v for a cylindrical nozzle (i.e. a potentially cavitating nozzle). The values have been normalized by the corresponding non-cavitating value.

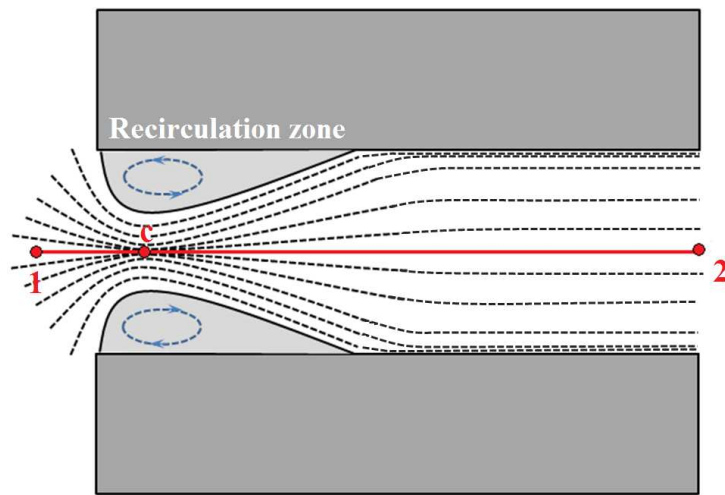


Figure 3: Schematics of the orifice configuration.

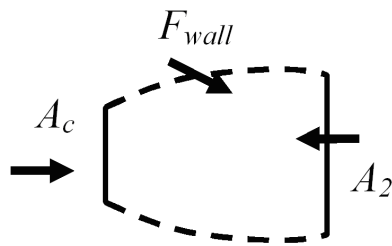


Figure 4: Control volume between sections c and 2 .

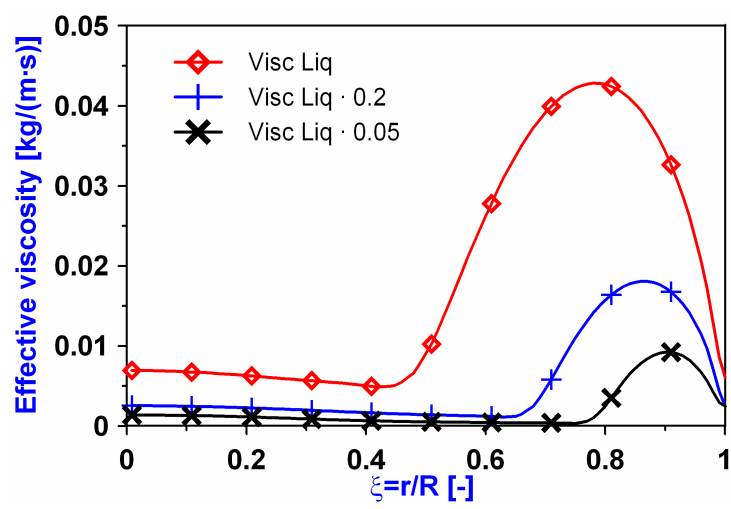


Figure 5: Effective viscosity profiles as a function of the normalized radial coordinate for the three viscosity levels simulated.

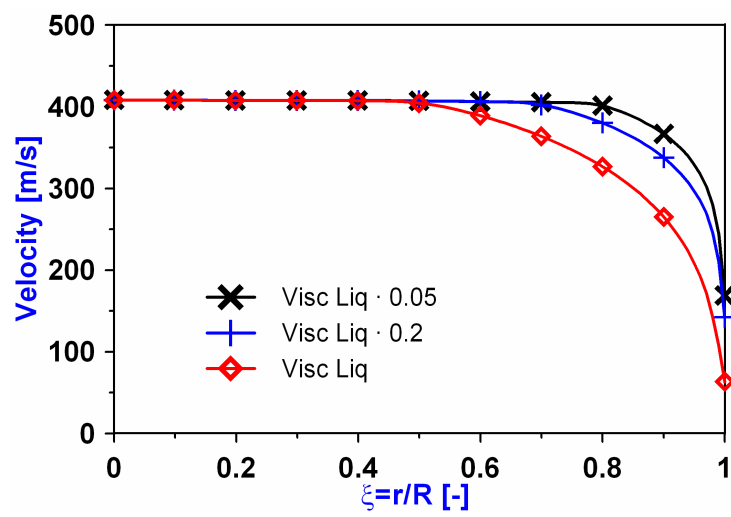


Figure 6: Velocity profiles as a function of the normalized radial coordinate for the three viscosity levels simulated.

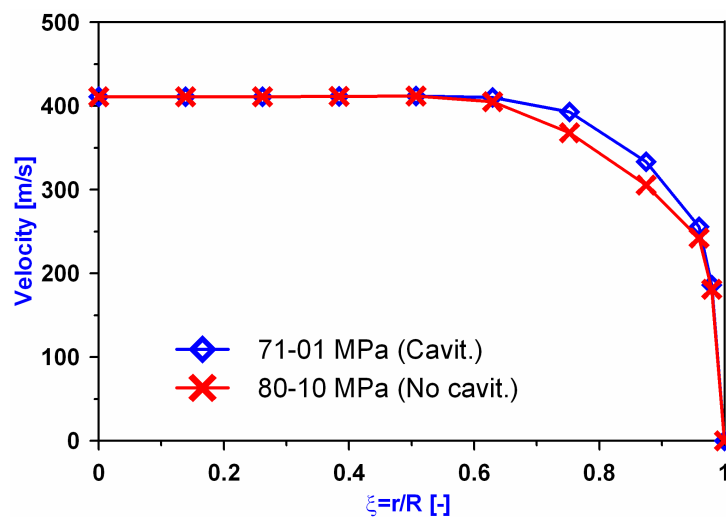


Figure 7: Velocity profiles as a function of the normalized radial coordinate for a cavitating and a non-cavitating case, both simulated with Star-CD using a cavitation model based in the Rayleigh equation.

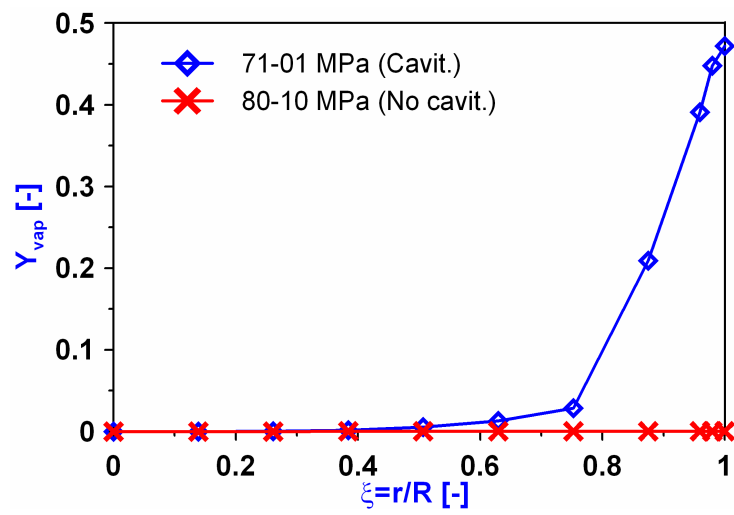


Figure 8: Evolution of the vapor mass fraction as a function of the normalized radial coordinate for the cases shown in Fig. 7.

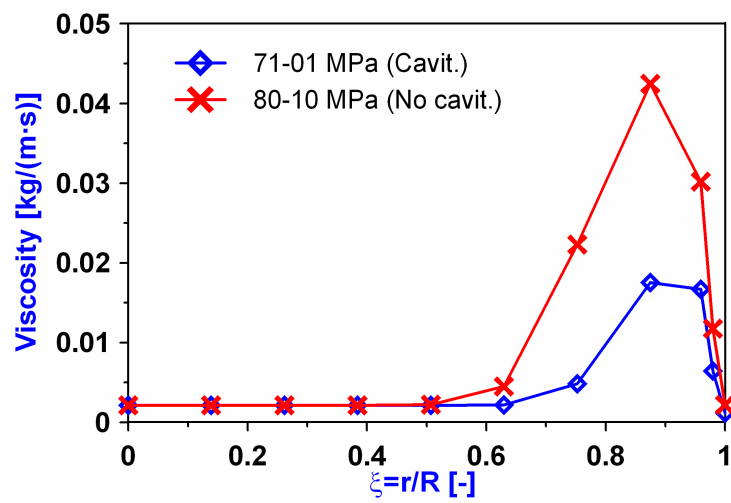


Figure 9: Evolution of the effective viscosity as a function of the normalized radial coordinate for the cases shown in Fig. 7.

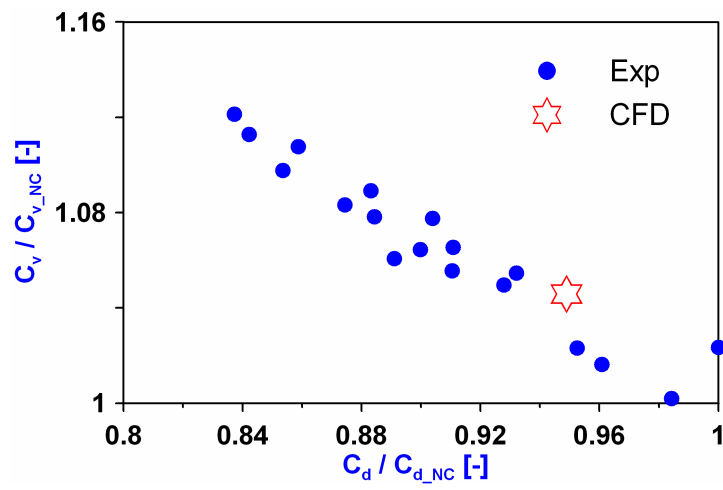


Figure 10: C_v versus C_d variations for the experimental cases shown in Fig.2. The same information for the CFD results is also shown.

List of Tables

1	Main characteristics and parameters of the performed simulations.	30
2	Effective velocity and its proportional change respect to the first case, and vapor mass fraction for the three viscosity levels.	31

Turbulence model	$k - \varepsilon$ RNG
Flow type	Incompressible
Orifice geometry	Conical (convergent)
Outlet diameter	112 μm
Outlet length	1 mm
Fluid density	835 kg/m^3
Fluid viscosity	$3.67 \cdot 10^{-3} / 7.34 \cdot 10^{-4} / 1.829 \cdot 10^{-4} \text{ } kg/(m \cdot s)$

Table 1: Main characteristics and parameters of the performed simulations.

Case	\dot{M}/\dot{m}	Ratio	Y_{vap}
	$[m/s]$	$[-]$	$[-]$
Liq. Viscosity	354.0	1.000	0
Liq. Viscosity $\times 0.2$	380.3	1.074	0.8
Liq. Viscosity $\times 0.05$	389.8	1.101	0.95

Table 2: Effective velocity and its proportional change respect to the first case, and vapor mass fraction for the three viscosity levels.